

Title	Helical frontier orbitals of conjugated linear molecules
Authors	Hendon, Christopher H.;Tiana, Davide;Murray, Alexander T.;Carbery, David R.;Walsh, Aron
Publication date	2013-01
Original Citation	Hendon, C. H., Tiana, D., Murray, A. T., Carbery, D. R. and Walsh, A. (2013) 'Helical frontier orbitals of conjugated linear molecules', Chemical Science, 4(11), pp. 4278-4284. doi: 10.1039/c3sc52061g
Type of publication	Article (peer-reviewed)
Link to publisher's version	<a href="http://pubs.rsc.org/en/content/articlepdf/2013/sc/c3sc52061g - 10.1039/c3sc52061g">http://pubs.rsc.org/en/content/articlepdf/2013/sc/c3sc52061g - 10.1039/c3sc52061g</a>
Rights	© The Royal Society of Chemistry 2013. This article is licensed under a Creative Commons Attribution 3.0 Unported Licence - <a href="https://creativecommons.org/licenses/by/3.0/">https://creativecommons.org/licenses/by/3.0/</a>
Download date	2024-02-23 19:23:15
Item downloaded from	<a href="https://hdl.handle.net/10468/6422">https://hdl.handle.net/10468/6422</a>

## Helical frontier orbitals of conjugated linear molecules

Cite this: *Chem. Sci.*, 2013, **4**, 4278

Christopher H. Hendon, Davide Tiana, Alexander T. Murray, David R. Carbery and Aron Walsh\*

Received 23rd July 2013  
Accepted 23rd August 2013

DOI: 10.1039/c3sc52061g

www.rsc.org/chemicalscience

## 1 Introduction

Allenes, cumulenes and oligoynes (polyalkynes) are intriguing structural motifs; they partake in cycloadditions, act as Michael acceptors and are redox active.<sup>1–6</sup> There has been a recent resurgence in studies relating to these molecules, as their inherent chirality, reactivity and unusual physical properties are useful in organic synthesis and as linking units in metal-organic frameworks (MOFs).<sup>7–11</sup>

Allene, **1**, is the most fundamental cumulated alkene; three carbons are bound linearly with double bonds. Through a basic molecular orbital construction of the  $\pi$ -system, the terminating motifs obtain an orthogonal conformation, Fig. 1. Allene may be axially chiral; the most simple example, 1,3-dimethyl allene, has two stereoisomers, (*M*) and (*P*). The next smallest cumulated alkene, cumulene (**2**), is planar by the same orbital description proposed for allene. The four carbons result in a planar molecule, achiral unless the terminating protons are substituted with a point chiral motif (*e.g.* (–)-menthol). A recent publication by Tykwinski and co-workers explored the structures of **2** and its extended variants, all of which had an *even* number of linear carbons and were achiral.<sup>8</sup> To the best of our knowledge, the most relevant studies of the next *odd* cumulene, containing five carbons, are related to interstellar diradicals, and other quasi-stable analogues.<sup>12–14</sup> There is no evidence to suggest that the *odd* cumulated alkenes are less stable than their *even* relatives, but rather that the previous synthetic routes do not yield odd catenated chains. There is scope for the synthesis of these molecules through some form of modified metathesis, but this has thus far not been explored.

Compounds containing allenes, cumulenes and oligoynes (polyalkynes) have attracted attention for both their conformation and reactivity. Whilst the textbook molecular orbital description explains the general electronic and molecular structure of the cumulenes, there are anomalies in both the crystal structures and cycloaddition products involving oligoynes and allenes; the understanding of these molecules is incomplete. Through a computational study we elucidate that the frontier orbitals of the allene and oligoyne families are extended helices. These orbitals are the linear analogue to the Möbius aromatic systems, which also display non-linear  $\pi$  interactions. The axial chirality found in allenes and oligoynes is intimately related to the topology of the frontier orbitals, and has implications for predictions of cycloaddition pathways, structure stability and spectroscopy.

The term ‘cumulene’ is not only the conventional molecular name of **2**, but is also used to refer to similar extended alkenes with four or more carbon atoms. This does not distinguish between the *odd* (**1**-like) and *even* (**2**-like) systems, or the molecule itself. Cumulenes like those described by Tykwinski and co-workers are *even* numbered and are thus planar ( $D_{2h}$ ) and pose no possibility for axial chirality. The *odd* cumulated alkenes are terminated in orthogonally-orientated functional motifs ( $D_{2d}$ ), and therefore may be axial chiral. In this work we refer to *odd* numbered cumulated alkenes as the family of ‘allenes’ and the *even* cumulated alkenes referred to as the family of ‘cumulenes’.

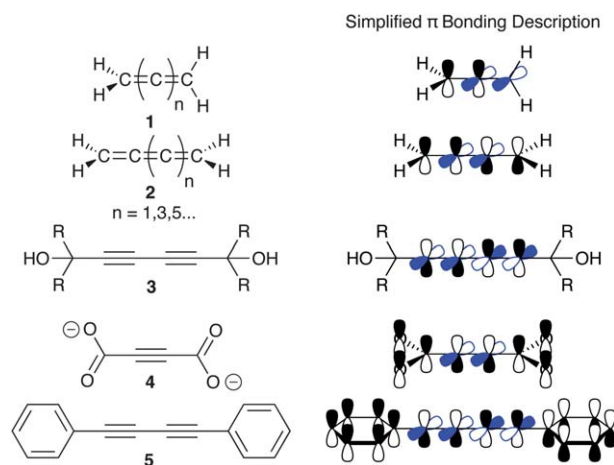


**Fig. 1** The archetype allene, **1**, and cumulene, **2**, with their simplified  $\pi$  bonding shown on the right. *Even* cumulated alkenes may be made from the hydrolysis of oligoynes similar to that of **3**. Related linear systems include the simple conjugated oligoyne, acetylene dicarboxylate, **4**, which is presumed planar, as is the aromatic terminated oligoyne, **5**.

Department of Chemistry, University of Bath, Claverton Down, Bath, BA2 7AY, UK.  
E-mail: a.walsh@bath.ac.uk; Tel: +44 (0)1225 384913



The cumulene family may be made by the two-electron oxidation of a cumulated alkyne precursor. Indeed the precursor alkynes, like that of **3**, share a similar electronic structure to their two-electron oxidised cumulene derivatives. Curiously, there have been a significant number of studies on extended conjugated oligoynes (ECOs), and their conformation; **4** and **5** are archetypes. It has been assumed that the orientation of the ECO family is planar like the cumulene family,<sup>15–18</sup> and some computational investigations have fixed this planarity through enforced  $D_{2h}$  symmetry.<sup>9,19</sup> Some studies *do* correctly suggest that ECOs demonstrate non-planar geometries: the terminating functional motifs rotate out of plane if they partake in the  $\pi$  conjugation of the alkyne.<sup>20,21</sup> This geometry is similar to that observed in the allene family, with one fundamental difference: ECOs have *even* numbers of carbon in the chain.

It is certainly less obvious why ECOs are structurally analogous to allenes. There are fleeting examples of such isolated structures; acetylene dicarboxylic acid has been observed in the orthogonal orientation in its crystal hydrate, seemingly stabilised through hydrogen bonding.<sup>22</sup> More recently, orthogonally-orientated oligoynes have been observed in MOFs, primarily as linking units.<sup>23,24</sup> IRMOF-0 (ref. 25) encompasses the ‘twisted’ acetylene dicarboxylate, **4**, and a similar MOF isolated by Burrows and co-workers features an orthogonal aromatic carboxylate terminated ECO.<sup>26</sup>

To understand the chemical similarities of the allenes and ECOs, and the differences between cumulenes and allenes, we must first understand the electronic structure of these molecules. Through quantum-chemical calculations we report on an unusual electronic characteristic in the allene and ECO families: *extended helical molecular orbitals*. The topology of these MOs has implications for predictions of cycloaddition products. The directed electronic structure is the linear analogue of the electronically chiral cyclic systems (canted  $\pi$  interactions) like that observed in Möbius aromatics.<sup>27</sup> Furthermore, it is these extended electronic helices which result in the observed orthogonality of the allene and ECO systems. The cumulene family displays no helical nature, further emphasising the difference between even and odd cumulated alkenes.

## 2 Electronic differences between the ‘odd’ allenes and ‘even’ cumulenes

The textbook MO construction of the  $\pi$  interactions between orthogonal atomic p-orbitals is sufficient to describe the electronic structure of the cumulenes. It is, however, inadequate in the description of the allenes. Quantum-chemical computations of these molecules confirm that the frontier molecular orbitals (FMOs) are comprised of p-orbitals for both systems, but perhaps not what one would expect. These are drawn schematically in Fig. 2 and formally in Fig. 4. *The allene family have extended FMOs with helical topology*. Through extended non-linear  $\pi$  interactions, allenes exhibit extended conjugation similar to that observed in Möbius aromatics, Fig. 2a, which are cyclic conjugated systems that feature the electronic topology of a Möbius ring.<sup>27</sup> The cumulenes show the expected p-orbital orthogonality with a centred node in the HOMO, Fig. 2b.

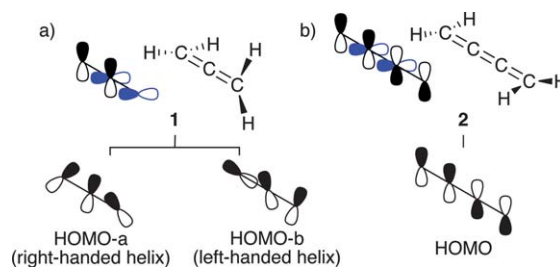


**Fig. 2** (a) Standard  $\pi$  bonding of allene assumes orthogonal  $\pi$  interactions. This description is insufficient as the HOMOs display non-orthogonality, resulting in extended helices. (b) Cumulenes are accurately described by textbook molecular orbital description.

The HOMO-*a* and *b* of the achiral allenes are a degenerate pair, comprised of the right and left-handed helices orientated  $90^\circ$  from each other. The rotation and polarisation of the p-orbitals of the central carbon atom results in this interesting electronic structure, with visibly helical molecular orbitals, Fig. 2a. The achiral allenes feature both the right and left-handed bias through electronic degeneracy. The splitting of this degeneracy may be achieved chemically by forming an axially chiral allene, thus differentiating the helical MOs.

Helical molecular orbitals can be observed in the cumulene family if the terminal motifs are non-planar. However, the equilibrium geometry of cumulenes is planar, and thus there is no potential for axial chirality. Even chemical substitution, *e.g.* methylation, does not induce non-planarity of the terminal motifs; therefore, there is no observed helical selectivity in organic reactions or in computational models.

The FMOs of the axially chiral (*P*)-1,3-dimethyl allene are shown in Fig. 4b; the degeneracy is removed upon substitutional methylation. The resulting MOs are helical; the HOMO of (*P*)-1,3-dimethyl allene is the left-handed helix. The HOMO-1 is found 0.002 eV below the HOMO, and is right-handed. Considering the other enantiomer, (*M*)-1,3-dimethyl allene, the HOMO is inverted to a right-handed helix. Contrast these helices to the molecular orbitals of a point chiral molecule: the chirality can be described by a non-linear asymmetric dipole about the stereogenic centre, like the direction and magnitude of the hands on a clock reading 01:45, Fig. 3a. A helix is the projection of this dipole through a third dimension, Fig. 3b.<sup>28</sup>

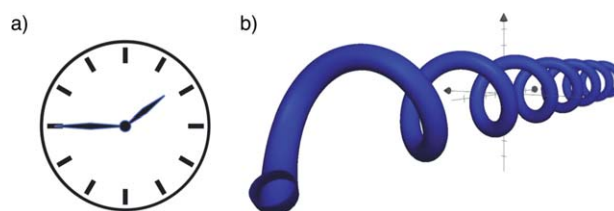


**Fig. 3** (a) The magnitude and direction of the clock hands are analogous to the dipoles of a point chiral molecule. (b) The projection of minute hands' displacement over time results in a helix, analogous to the extended helices observed in the linear molecules discussed herein.



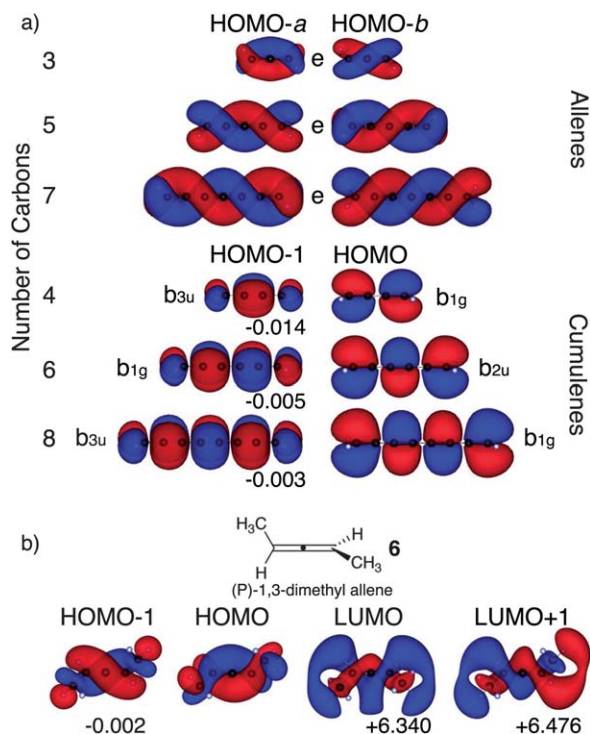


**Fig. 4** Frontier orbitals calculated using density functional theory. (a) Odd numbered allenes demonstrate helical degenerate orbitals of symmetry *e*, whilst their even numbered analogues, the cumulenes, obtain the usual orthogonality with the orbital symmetries labelled. (b) The axially chiral (*P*)-1,3-dimethyl allene maintains the helical characteristics in both the HOMO (left-handed helix) and the HOMO-1 (right-handed helix). The two virtual orbitals, LUMO and LUMO+1, are left and right-handed, respectively. The energies are described in eV and relative to the corresponding HOMO. The orbital depictions are from the wavefunctions calculated with the TPSSh functional with the isovalue set to 0.015 e<sup>Å</sup><sup>-3</sup>.

These linear molecules are unusual because they maintain both chiral identities in their molecular orbitals. The helical nature of the allene orbitals is best observed, but not limited to, the FMOs. For axially chiral allenes, like those shown in Fig. 4b, it is important to note that the 'handedness' of the HOMO and LUMO are the same (and opposite to that of the HOMO-1 and LUMO+1).

Helicity is a familiar structural topology in organic chemistry,<sup>29-33</sup> a familiar example is the helicene family.<sup>34-36</sup> Logically, the HOMO is composed of the highest energy occupied linear combination of atom-centred orbitals and is intimately related to the molecular geometry. For conventionally chiral systems there is no HOMO-*n* that reflects the opposite enantiomer. Considering the helicenes, there is structurally only one electronic enantiomer present. In linear molecules, like the allenes, both identities are portrayed, further lamenting the unique behaviour of the helical FMOs explored herein.

There is experimental precedence for the existence of helical molecular orbitals.<sup>37-39</sup> Consider the familiar [2 + 2] cycloaddition described in Fig. 5. In a general sense, the occupied orbitals of **7** interact with the unoccupied orbitals of **8** forming a cyclobutane. The criteria for such reactions vary. Some require irradiation to promote the reaction of the first excited state of the electron acceptor (**8**), others are thermally favourable. There

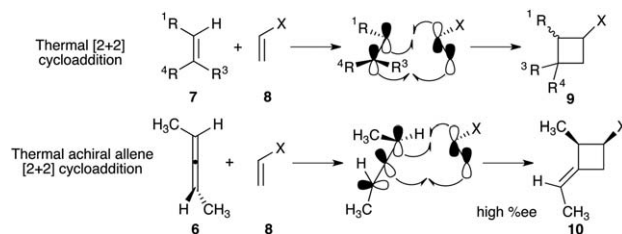


**Fig. 5** The familiar orbital description of a thermal [2 + 2] cycloaddition reaction. This reaction is non-concerted but follows the general description depicted top-right. Achiral allenes react through their HOMO-*a/b*, with no inherent enantiomeric selectivity.

are many examples of allenes partaking in similar reactions, best summarised in the recent review by Alcaide and co-workers.<sup>7</sup> There are accounts of allenes partaking in [3 + 2] cycloadditions (acting as the 3 component) through either in the presence of a nucleophilic organocatalyst<sup>40,41</sup> or a metal catalyst.<sup>42,43</sup> In such instances, an enolate is formed, subsequently racemising the allene. It is rather the [even + even] cycloadditions that demonstrate the application of such helical FMOs.

The allene cycloaddition reactions obey the Woodward-Hoffmann rules,<sup>44-46</sup> but the general consensus is that these cycloadditions are not concerted.<sup>7</sup> In [even + even] cycloadditions involving chiral allenes, there are many reports of enantioselectivity in the formation of radical intermediates. Two intriguing examples are the thermal [2 + 2] of **6** and methyl propiolate,<sup>47</sup> and a more complex [2 + 2] intramolecular photocycloaddition.<sup>48</sup> In both instances single molecule calculations affirm that the HOMOs are 'left-handed'.

Previously, high selectivity in cycloadditions involving chiral allenes was rationalised through steric preferences of the reagents.<sup>47</sup> This is almost certainly not the case; whilst the interacting geometry is of thermodynamic importance, the enantioselectivity is the product of orbital symmetry conservation (*i.e.* the symmetry of the HOMO of the allene in relation to the LUMO of **8** is allowed). Fig. 6a describes a proposed symmetry-allowed in-phase orbital reorientation, which is intimately related to the 'handedness' of the allene HOMO. This is in contrast to the symmetry-forbidden p-orbital reorientation shown in Fig. 6b, where the extended conjugation is broken rapidly. Therefore, the application of the helical molecular orbital description provides insight into the predictions of cycloaddition reactions and accurately describes the observed high enantioselectivity. Indeed, the products of the

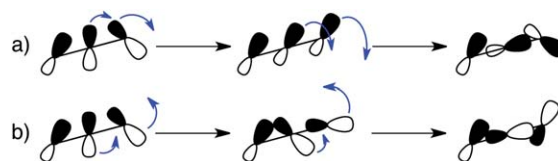


**Fig. 6** (a) Orbital restructuring in accordance to the conservation of symmetry: *unwinding of the helix*. (b) Orbital restructuring resulting in a change in symmetry, violating the Woodward-Hoffmann rules: *over-winding of the helix*.



cycloaddition reflect the orbital symmetry of the precursors, allowing the heuristic prediction of the electronic structure of the allene precursor. This may become more important once large *odd* cumulated alkenes are synthesised and used in similar reactions.

### 3 Extended conjugated oligoynes

Unlike the allenes and cumulenes, which are orthogonal and planar, respectively, the geometries of ECOs exhibit more variation.<sup>49</sup> The simplest ECO, acetylene dicarboxylate (**4**), and the ester derivative, are generally considered to be planar, resulting in a non-degenerate HOMO/HOMO–1 due to the inequivalent  $\pi_x$  and  $\pi_y$  interactions.<sup>15–18</sup>

The generalised family of ECOs are shown in Fig. 7. The ECO equilibrium geometry can be found by rotation of the conjugated terminating groups (carboxylate torsion angle; CTA). The potential energy surface has been constructed for the archetype ECO systems, Fig. 8. The acetylene dicarboxylate (**4**) orbital images accompanying the PES illustrate the HOMOs at the local maximum (CTA = 0°,  $D_{2h}$  symmetry), twist transition (CTA = 45°,  $D_2$  symmetry) and the global minimum (~90°,  $D_2$ , near  $D_{2d}$ , symmetry). The global minimum was found through both an unconstrained optimisation of **4**, **11** and **12** (depicted as shaded points in Fig. 8), and the fixed CTA calculations used to construct the PES. Very good agreement between the calculated and experimental bond lengths is observed, with a difference of the order  $10^{-2}$  Å. All of the molecules described in Fig. 7, and their structural analogues, have non-planar global minima.

A near orthogonal conformation (CTA = 87.28°/92.72°) is energetically favourable for the monoalkyne system, **4**, with a 10.33 kJ mol<sup>-1</sup> energy stabilisation over the planar variation. A similar trend is observed for the larger oligoynes, **11** (CTA = 88.76°/91.24°) and **12** (CTA = 89.88°/90.12°), with 4.99 and 2.96 kJ mol<sup>-1</sup>, respectively. It is notable that both the planar and orthogonal conformations are saddle points (both  $D_{2h}$  and  $D_{2d}$  prevent the formation of the helices). As catenation is increased, the barrier of rotation is reduced and the global minimum converges to the orthogonal conformation, CTA = 90°. The origins of the unfavourable planar geometry are the combination of repulsive interactions between the terminating functional groups (visualised in the PES, CTA = 0°) and the constructive orbital overlap, similar to the Möbius systems, upon twisting (Fig. 9). Thus for different reasons, extended conjugated oligoynes obtain a similar geometry to that of the allene family,

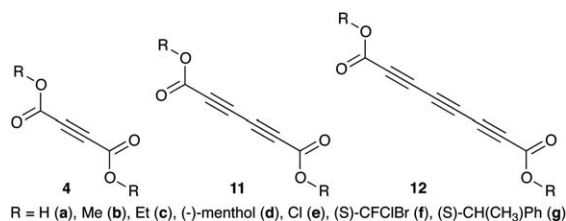


**Fig. 7** Extended conjugated oligoynes and their variable terminating motifs. In the case where R is excluded the systems are considered as the di-anion.

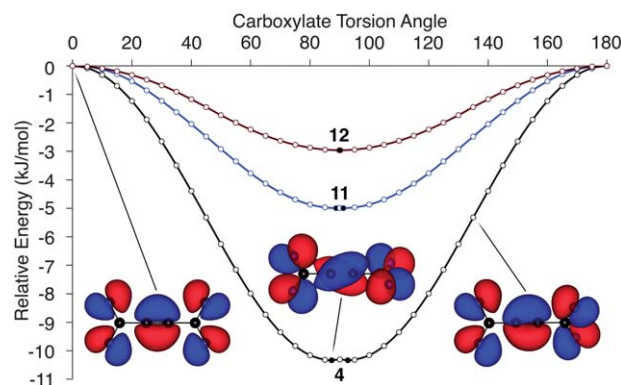


**Fig. 8** Potential energy surfaces of **4**, **11** and **12** at the DFT-TPSSH level of theory. The optimised geometry is shown by the shaded points. MO images are from the optimised structures of CTA = 0°, 50° and ~90° (shaded point). The isosurface value is set to 0.025 eÅ<sup>-3</sup>.

with one important difference: all extended conjugated oligoynes are made up of *even* numbered carbon chains.

The structural twist is observed in all of the ECO series; selected examples are shown in Fig. 9. The electronic result is the formation of a degenerate extended helical  $\pi$  system similar

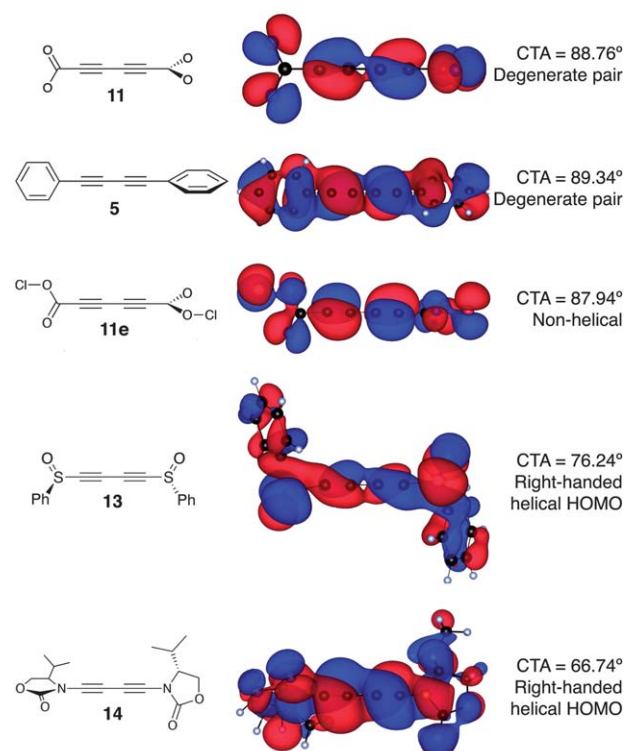


**Fig. 9** Depicted are the highest occupied MOs (DFT-TPSSH), and carboxylate torsion angle, of five extended conjugated oligoynes. **11** and **5** are fundamental ECOs with optimised CTA near 90°. Rehybridisation of oxygen in **11e** removes the helical nature of the compound, but the orthogonal arrangement is still favourable. **13** (a dialkyne terminated in (*R*)-phenylsulfanyl) displays a right-handed HOMO (CTA defined through the O–S–S–O angle). **14** (a dialkyne terminated in (*R*)-4-isopropyl-oxazolidin-2-one) displays a right-handed HOMO (CTA defined through the O–N–N–O angle). Isosurface value = 0.025 eÅ<sup>-3</sup>.



to that of allene. In addition to the occupied electronic orbitals, most virtual orbitals are also helical in nature. The lowest-unoccupied molecular orbital is helical and degenerate. These helices are more robust than the HOMO orbitals with respect to chemical substitution; we have not discovered a oligoyne terminating in *any* conjugated motif that removes the extended helical nature of the orbitals. This finding may become important when exploring optical excitations, and have interesting implications for cycloaddition reactions.

Similar to the cumulenes, an approach for creating inequivalent right and left-handed helices in oligoynes is the installation of a point chiral motif, Fig. 7d, f and g.<sup>50</sup> The fundamental problem with a chiral ester functionality is that the alkoxy oxygen is no longer formally part of the conjugated system. Effective removal of the helical  $\pi$ -system can be achieved by attaching electron-withdrawing groups (e.g.  $-\text{Cl}$ , shown schematically in Fig. 7e and formally in Fig. 9) or an organic molecule (e.g.  $-\text{Me}$ , Fig. 7a–d) to the terminal oxygen atoms. The reduction in conjugation is a product of the re-hybridisation of oxygen, removing  $\pi$  overlap with the alkyne chain. Extended electronic helices observed in **5**, and relevant derivatives, are affected to a lesser extent by substituents on the ring. Depending on the substituent, strongly electron withdrawing groups, like the carboxylic acids, cause the helical MOs to appear in the HOMO–5 to HOMO–8 region.

An alternative approach is the substitution of the terminal carbons for chiral sulfoxides or oxazolidinones. We have proposed the *R*-phenylsulfinyl substituent as a conjugated alternative to carboxylate termini (as shown by **13**, Fig. 9d). It is not necessary for the ‘dangling’ substituents to be conjugated to the oligoyne. In this instance, the conjugation in the sulfoxide is extended. By the addition of the point chiral motif, the oligoyne HOMOs are split, again reflecting the chirality of the system. In this case, the separation of the HOMO (right-handed helix) and HOMO–1 (left-handed helix) is  $\sim 0.02$  eV. One promising example is the oxazolidinone described in Fig. 9e. The nitrogen acts similar to the sulfur in this instance, conjugating to the alkyne motifs and, more importantly, providing a bias for the helices. The specific oxazolidinone, (*R*)-4-isopropylloxazolidin-2-one (**14**), is both synthetically plausible, and, like the sulfoxide, can be isolated in a solid (similar to presence of **4** in MOFs).<sup>51–53</sup> Single-molecule calculations of **14** result in a 0.42 eV energy separation of the HOMO and HOMO–1.

The chiral oxazolidinone and sulfoxide demonstrate a separation of degenerate orbitals in the ECO family. The attachment of these conjugated oligoynes amplifies the effect of point chirality, and should be detectable spectroscopically. With respect to reactivity, the oligoynes may act as both the electron accepting and donating motifs. The cycloaddition discussion for allenes is applicable to oligoynes; however, the isolation of a single helix remains an area that has yet to be thoroughly explored. In principle, the kinetic product of the chiral oligoyne [2 + 2] cycloaddition reaction should reflect a similar outcome to the allenes; the helical conformation is thermodynamically favoured. There should be chiral selectivity in cycloadditions involving the oxazolidinone (the HOMO is helical and separated by 0.42 eV from the inverse HOMO–1).

There are ECOs that do not exhibit extended helices. A contemporary example is porphyrin systems linked by diynes,<sup>54</sup> where there are two interactions that disfavour the formation of the orthogonal structure and thus helical orbitals. Firstly, the tetrahedral Zn ions interact with the porphyrin, altering the hybridisation of the alkyne/porphyrin orbitals. Secondly, the extended conjugation is terminated with unconjugated silyl motifs. As demonstrated here, unconjugated motifs remove the extended helicity. The planar conformation is still conventionally conjugated in the equilibrium geometry; the HOMO and HOMO–1 consist of nodes not observed in the extended helices of orthogonal ECOs.

## 4 Conclusion

The description of both the orbital structures of the allenes and extended conjugated oligoynes, and the reactivity of these motifs is incomplete. Herein we have described the distinct electronic structure of the allene and extended conjugated oligoyne families; both the allenes and the ECOs display extended helical frontier orbitals. Whilst these extended helices are degenerate in the unsubstituted systems, chemically activated chirality (distinct right and left-handed helices) may be preferentially performed through intelligent design.

Our results justify the observed structural orthogonality in allenes and ECOs. The orthogonality of the ECOs is the result of the conformation being in a potential energy minimum, a stabilisation due to the formation of extended helices. The allenes are inherently structurally orthogonal, but display similar helical orbitals. This helical nature provides a rigorous explanation for enantioselectivity in cycloadditions involving chiral allenes. The helicity found in the ECOs is predicted to be observable spectroscopically and in enantioselective cycloadditions. Furthermore, these structures are ones of importance with applications as both ligands and guest molecules in metal-organic frameworks. Their rigidity and potential optical response makes them interesting ligand candidates.

Importantly, we have also demonstrated a fundamental difference between the cumulenes and allenes. The cumulene family (even numbered carbons) are planar and do not display helical MOs, whilst the allene family (odd numbered carbons) are orthogonally terminated and display electrohelicity. The distinct behaviour further laments that molecular orbitals are not always what they appear; indeed, an ending with a twist.

Since our original submission, an investigation of the mechanical properties of extended conjugated systems has been reported,<sup>55</sup> which identifies a periodic torsional response consistent with the canted  $\pi$  interactions that we observe.

## 5 Computational details

All quantum chemical calculations were performed using the GAMESS-US package.<sup>56</sup> The atomic geometries were optimised within the Kohn–Sham density functional theory (DFT)<sup>57</sup> construct. The total energy and forces were calculated with the hybrid meta-generalised gradient approximation functional, TPSSH,<sup>58</sup> using a triple zeta basis set, 6-311+G(3d).<sup>59</sup> The



potential energy surfaces were obtained by relaxing the internal coordinates as a function of the dihedral angle between the terminal groups. A range of semi-local and non-local exchange-correlation functionals (e.g. PBE,<sup>60</sup> PBE0,<sup>61</sup> M06 (ref. 62)) and a wave function based method (MP2)<sup>63</sup> were found to give similar predictions.

To ensure quantitative results, the electronic structure and internal energies were also calculated for select systems at the coupled cluster level of theory including single, double and perturbative triple excitations, CCSD(T),<sup>64,65</sup> with the same basis set. The potential energy surfaces and molecular orbitals show very good agreement with the TPSSH results, with the exception that the barriers for rotation for the oligoynes are slightly reduced (+2 kJ mol<sup>-1</sup> for **4**), which is consistent with a more rigorous description of electron correlation.<sup>66</sup> Visualisations of the structures and orbitals were made using the codes VESTA and GABEDIT.<sup>67,68</sup>

## Acknowledgements

We thank A. D. Burrows for useful discussions. A.W. is supported a Royal Society University Research Fellowship, while C.H.H. and D.T. are funded under ERC Starting Grant 277757. A.T.M. is supported by the University of Bath while D.R.C. is funded by EPSRC (Grant no. EP/K004956/1). The work benefited from the University of Bath's High Performance Computing Facility, and access to the HECToR supercomputer through membership of the UK HPC Materials Chemistry Consortium, which is funded by EPSRC (Grant no. EP/F067496).

## References

- 1 R. Bonjouklian and R. Ruden, *J. Org. Chem.*, 1977, **42**, 4095.
- 2 N. Saito, T. Ichimaru and Y. Sato, *Chem.-Asian J.*, 2012, **7**, 1521.
- 3 M. S. Shafawati, F. Inagaki, T. Kawamura and C. Mukai, *Tetrahedron*, 2013, **69**, 1509.
- 4 F. Inagaki, H. Kobayashi and C. Mukai, *Chem. Pharm. Bull.*, 2012, **60**, 381.
- 5 A. Fukazawa, H. Oshima, Y. Shiota, S. Takahashi, K. Yoshizawa and S. Yamaguchi, *J. Am. Chem. Soc.*, 2013, **135**, 1731.
- 6 D. Uraguchi, Y. Ueki, A. Sugiyama and T. Ooi, *Chem. Sci.*, 2013, **4**, 1308.
- 7 B. Alcaide, P. Almendros and C. Aragoncillo, *Chem. Soc. Rev.*, 2010, **39**, 783.
- 8 J. A. Januszewski, D. Wendinger, C. D. Methfessel, F. Hampel and R. R. Tykwinski, *Angew. Chem., Int. Ed.*, 2013, 1817.
- 9 S. Ohashi and S. Inagaki, *Tetrahedron*, 2001, **57**, 5361.
- 10 S.-i. Kato, N. Takahashi and Y. Nakamura, *J. Org. Chem.*, 2013, **78**, 7658–7663.
- 11 Y. Li, M. E. Köse and K. S. Schanze, *J. Phys. Chem. B*, 2013, **117**, 9025.
- 12 N. P. Bowling, R. J. Halter, J. A. Hodges, R. A. Seburg, P. S. Thomas, C. S. Simmons, J. F. Stanton and R. J. McMahon, *J. Am. Chem. Soc.*, 2006, **128**, 3291.
- 13 C. Liang, Y. Xie, H. F. Schaefer III, K. S. Kim and H. S. Kim, *J. Am. Chem. Soc.*, 1991, **113**, 2452.
- 14 J. Ripoll, *J. Chem. Soc., Chem. Commun.*, 1976, 235.
- 15 T. W. Abbott, R. T. Arnold and R. B. Thompson, *Org. Synth.*, 1938, **18**, 3.
- 16 J. L. Charlton, G. Chee and H. Mccoleman, *Can. J. Chem.*, 1995, **73**, 1454.
- 17 V. Y. Kauss, E. E. Liepin'sh, I. Y. Kalvin'sh and E. Lukevits, *Chem. Heterocycl. Compd.*, 1990, **26**, 103.
- 18 B. Zheng, J. Luo, F. Wang, Y. Peng, G. Li, Q. Huo and Y. Liu, *Cryst. Growth Des.*, 2013, **13**, 1033.
- 19 Y. Nagano, T. Ikoma, K. Akiyama and S. Tero-Kubota, *J. Am. Chem. Soc.*, 2003, **125**, 14103.
- 20 S. Menning, M. Krämer, B. A. Coombs, F. Rominger, A. Beeby, A. Dreuw and U. H. F. Bunz, *J. Am. Chem. Soc.*, 2013, **135**, 2160.
- 21 B. L. J. Poad, B. B. Kirk, P. I. Hettiarachchi, A. J. Trevitt, S. J. Blanksby and T. Clark, *Angew. Chem., Int. Ed.*, 2013, **52**, 9301.
- 22 J. D. Dunitz and J. M. Robertson, *J. Chem. Soc.*, 1947, 1145.
- 23 O. K. Farha, C. D. Malliakas, M. G. Kanatzidis and J. T. Hupp, *J. Am. Chem. Soc.*, 2010, **132**, 950.
- 24 H. Furukawa, N. Ko, Y. B. Go, N. Aratani, S. B. Choi, E. Choi, a. O. Yazaydin, R. Q. Snurr, M. O'Keeffe, J. Kim and O. M. Yaghi, *Science*, 2010, **329**, 424.
- 25 D. Tranchemontagne, J. Hunt and O. Yaghi, *Tetrahedron*, 2008, **64**, 8553.
- 26 A. D. Burrows, L. C. Fisher, D. Hodgson, M. F. Mahon, N. F. Cessford, T. Düren, C. Richardson and S. P. Rigby, *CrystEngComm*, 2012, **14**, 188.
- 27 Z. S. Yoon, A. Osuka and D. Kim, *Nat. Chem.*, 2009, **2**, 113.
- 28 D. Z. Wang, *Tetrahedron*, 2005, **61**, 7125.
- 29 S. Hedström and P. Persson, *J. Phys. Chem. C*, 2012, **116**, 26700.
- 30 M. R. Crittall, N. W. G. Fairhurst and D. R. Carbery, *Chem. Commun.*, 2012, **48**, 11181.
- 31 V. Murphy and B. Kahr, *J. Am. Chem. Soc.*, 2011, 12918.
- 32 M. R. Crittall, H. S. Rzepa and D. R. Carbery, *Org. Lett.*, 2011, **13**, 1250.
- 33 D. Kitagawa, H. Nishi and S. Kobatake, *Angew. Chem., Int. Ed.*, 2013, **52**, 9320.
- 34 M. Gingras, *Chem. Soc. Rev.*, 2013, **42**, 968.
- 35 M. Gingras, G. Félix and R. Peresutti, *Chem. Soc. Rev.*, 2013, **42**, 1007.
- 36 M. Gingras, *Chem. Soc. Rev.*, 2013, **42**, 1051.
- 37 M. R. Siebert, J. M. Osbourn, K. M. Brummond and D. J. Tantillo, *J. Am. Chem. Soc.*, 2010, **132**, 11952.
- 38 A. D. Allen and T. T. Tidwell, *Chem. Rev.*, 2013, DOI: 10.1021/cr3005263, in press.
- 39 D. Campolo, S. Gastaldi, C. Roussel, M. P. Bertrand and M. Nechab, *Chem. Soc. Rev.*, 2013, DOI: 10.1039/c3cs60182j, in press.
- 40 J. E. Wilson and G. C. Fu, *Angew. Chem., Int. Ed.*, 2006, **45**, 1426.
- 41 X. Han, Y. Wang, F. Zhong and Y. Lu, *J. Am. Chem. Soc.*, 2011, **133**, 1726.



- 42 H.-T. Chang, T. T. Jayanth and C.-H. Cheng, *J. Am. Chem. Soc.*, 2007, **129**, 4166.
- 43 P. Mauleón, R. M. Zeldin, A. Z. González and F. D. Toste, *J. Am. Chem. Soc.*, 2009, **131**, 6348.
- 44 R. B. Woodward and R. Hoffmann, *J. Am. Chem. Soc.*, 1965, **1**, 395.
- 45 R. B. Woodward and R. Hoffmann, *Angew. Chem., Int. Ed.*, 1969, **8**, 781.
- 46 R. Hoffmann and R. B. Woodward, *Acc. Chem. Res.*, 1968, **1**, 17.
- 47 D. J. Pasto, K. D. Sugi and D. E. Alonso, *J. Org. Chem.*, 1992, **57**, 1146.
- 48 E. Carreira, C. Hastings, M. Shepard, L. Yerkey and D. Millward, *J. Am. Chem. Soc.*, 1994, **116**, 6622.
- 49 S. T. Li, T. Schnabel, S. Lysenko, K. Brandhorst and M. Tamm, *Chem. Commun.*, 2013, **49**, 7189.
- 50 B. C. Ranu, A. Sarkar, M. Saha and S. Bhar, *Pure Appl. Chem.*, 1996, **68**, 775.
- 51 Y. Li, G. Xu, W.-Q. Zou, M.-S. Wang, F.-K. Zheng, M.-F. Wu, H.-Y. Zeng, G.-C. Guo and J.-S. Huang, *Inorg. Chem.*, 2008, **47**, 7945.
- 52 M. Owczarek, P. Szklarz, R. Jakubas and A. Miniewicz, *Dalton Trans.*, 2012, **41**, 7285.
- 53 D. A. Links, Z.-Y. Liu, B. Ding, E.-C. Yang and X.-j. Zhao, *Dalton Trans.*, 2012, **41**, 9611.
- 54 M. Winters, J. Kärnbratt, M. Eng, C. J. Wilson, H. L. Anderson and B. Albinsson, *J. Phys. Chem. C*, 2007, **111**, 7192.
- 55 M. Liu, V. I. Artyukhov, H. Lee, F. Xu and B. I. Yakobson, 2013, arXiv: 1308:2258.
- 56 M. W. Schmidt, K. K. Baldrige, J. A. Boatz, S. T. Elbert, M. S. Gordon, J. H. Jensen, S. Koseki, N. Matsunaga, K. A. Nguyen, S. Su, T. L. Windus, M. Dupuis and J. A. Montgomery, *J. Comput. Chem.*, 1993, **14**, 1347.
- 57 P. Hohenberg and W. Kohn, *Phys. Rev.*, 1964, **155**, 864.
- 58 J. Tao, J. Perdew, V. Staroverov and G. Scuseria, *Phys. Rev. Lett.*, 2003, **91**, 3.
- 59 R. Krishnan, J. S. Binkley, R. Seeger and J. A. Pople, *J. Chem. Phys.*, 1980, **72**, 650.
- 60 J. P. Perdew, K. Burke and M. Ernzerhof, *Phys. Rev. Lett.*, 1996, **77**, 3865.
- 61 C. Adamo and V. Barone, *Chem. Phys. Lett.*, 1998, 113.
- 62 Y. Zhao and D. G. Truhlar, *Theor. Chem. Acc.*, 2007, **120**, 215.
- 63 C. Moller and M. Plesset, *Phys. Rev.*, 1934, **240**, 618.
- 64 H. Koch and P. Jorgensen, *J. Chem. Phys.*, 1990, **93**, 3333.
- 65 T. H. Dunning, *J. Chem. Phys.*, 1989, **90**, 1007.
- 66 M. Barborini and L. Guidoni, *J. Chem. Phys.*, 2012, **137**, 224309.
- 67 K. Momma and F. Izumi, *J. Appl. Crystallogr.*, 2011, **44**, 1272.
- 68 A.-R. Allouche, *J. Comput. Chem.*, 2010, 174.

